A Density Functional Theory Study of a Silica-Supported Zirconium Monohydride Catalyst for Depolymerization of Polyethylene

Jens Jørgen Mortensen* and Michele Parrinello

Max-Planck-Institut für Festkörperforschung, Heisenbergstr. 1, 70569 Stuttgart, Germany

Received: November 16, 1999

A silica-supported zirconium hydride catalyst for depolymerization of polyethylene is studied using density functional theory (DFT) together with a generalized gradient approximation (GGA) for the exchange and correlation energy. The (100) and (111) surfaces of β-cristobalite are used as two possible models of a silica surface. Based on the experimental surface structure determined by J. Corker et al. (*Science* **1996**, *271*, 966), we propose a detailed atomic model of the zirconium monohydride that is believed to be the active site for depolymerization of polyolefins. Our model of the zirconium monohydride on the (100) surface is found to be very stable and the structure is in good agreement with extended X-ray absorption fine structure (EXAFS) measurements. We have carried out depolymerization of a small polyolefin chain (C_3H_8) to give CH_4 and C_2H_6 by addition of H_2. The rate-limiting step is a β-methyl transfer to the zirconium atom, and the activation energy is 29 kcal/mol on the (100) surface.

1. Introduction

Conversion of waste plastics, such as polyolefins, into reusable chemicals is of great economical and environmental interest.[1] Such conversions are expensive due to the high temperatures needed. Typically, hydrogenation of polyolefins to give alkanes is carried out at high temperatures and high hydrogen pressures (∼500 °C and ∼100 atm).[2] Recently, Basset and co-workers have used as catalyst zirconium monohydride supported on a surface of silica−alumina and found that it is capable of cleaving C−C bonds in several simple alkanes under milder conditions.[3] For instance, on a surface of pure silica, neopentane is converted into ethylene and methane after hours at 25 °C and a hydrogen pressure of 1 atm.[4] On a silica−alumina substrate the catalyst is even more reactive.[5]

While we are not aware of any theoretical studies of the microscopic reaction mechanism of catalytic depolymerization, the related subject Ziegler−Natta (ZN) polymerization[6−13] is one of the most studied chemical reactions since its discovery in 1953.[14] The key step in ZN polymerization is an olefin insertion into a metal−alkyl bond which is the reverse of the step leading to depolymerization, namely the β-alkyl transfer.[3] With modern computational methods based on density functional theory (DFT)[15,16] and the Car−Parrinello method it has recently become possible to study the problem of ZN catalysis in its complexity, including a realistic description of the surfaces.[12] In this work we apply the same method to the depolymerization process discovered by Basset. We have here the additional difficulty that the surface structure of silica is insufficiently known. Unfortunately, an ab initio determination of the silica surface is beyond present day capability.[17,18] For this reason, following other authors, we shall use, as model for the local surface environment, the (100) and (111) surfaces of the β-cristobalite polymorph of SiO_2, which has approximately the same density as amorphous silica.

In contrast, the local structure of of the zirconium monohydride has been determined by Corker et al.[4] using a combination of extended X-ray absorption fine structure (EXAFS), ^{1}H and ^{29}Si solid-state nuclear magnetic resonance and infrared spectra. Our calculation shows that this structure is indeed stable, confirming the interpretation of Corker et al.

Our main interest is to study the energetics of a depolymerization reaction on a silica-supported zirconium monohydride, to provide the insight needed to improve the process. However, we believe that our results will also be relevant for other types of depolymerization catalysts or completely different reactions on silica surfaces.

2. Experimental Facts about the Zirconium Monohydride Catalyst

From a large number of experimental techniques, the following can be summarized about the preparation of the catalyst.[3−5]

Step 1: The first step in the preparation of the catalyst is room-temperature adsorption of tetraneopentylzirconium ($ZrNp_4$, $Np = CH_2C(CH_3)_3$) on a silica surface dehydroxylated at 500 °C. For each molecule that reacts with a silanol (≻SiOH or simply OH group), a neopentane molecule (NpH) is released leaving a $\succ SiOZrNp_3$ species on the surface.

$$\succ SiOH + ZrNp_4 \rightarrow \succ SiOZrNp_3 + NpH \qquad (1)$$

Step 2: Under hydrogen pressure at 150 °C a zirconium monohydride, that can be characterized as $(\succ SiO)_3ZrH$, is formed. At the same time infrared data showed indications of a silicon dihydride species ($>SiH_2$).

$$\succ SiOZrNp_3 + (\succ SiO)_2Si< + 3H_2 \rightarrow (\succ SiO)_3ZrH + >SiH_2 + 3NpH \qquad (2)$$

The fact that the zirconium atom is coordinated to three oxygen atoms (Zr−O bond lengths 1.95 Å) and that $>SiH_2$ is

* Author to whom correspondence should be addressed. E-mail: morten@prr.mpi-stuttgart.mpg.de.

10.1021/jp994056v CCC: $19.00
Published on Web 03/14/2000

formed led Corker et al.[4] to suggest the following more detailed mechanism for step 2 above: The ≥SiOZrNp$_3$ is hydrogenolyzed, giving an intermediate state ≥SiOZrH$_3$. The zirconium atom of this complex approaches a silicon atom of a neighboring SiO_4 tetrahedron, thereby breaking two Si−O bonds and two Zr−H bonds, simultaneously forming two Zr−O bonds and two Si−H bonds giving (≥SiO)$_3$ZrH and >SiH$_2$ (see Figures 3 and 4 of this paper or Scheme 1 in ref 4). This information will be very useful when we start looking for a possible structural model of the catalyst.

3. Methods

To approximate an infinite surface we shall use a periodically repeated slab. Its dimension in the *x, y* directions are 10.1 × 10.1 Å and 10.1 × 8.7 Å for the (100) and (111) surfaces which correspond to (2 × 2) and c(4 × 2) surface unit cells, respectively. The dimension of the supercell in the direction perpendicular to the surface is 25 Å. The (100) and (111) silica unit cells contain 46 and 36 atoms, respectively, which correspond to approximately 7 Å thick slabs, and the density functionals used for exchange and correlation are those of Becke[19] and of Lee et al.,[20] respectively. Core electrons are treated with pseudopotentials developed by Goedecker et al.[21,22] For zirconium we have treated the semi-core orbitals 4s and 4p explicitly. The slab is decoupled from its images using the scheme of Martyna and Tuckerman.[23]

The pseudopotential for oxygen is very hard and a plane wave cutoff of 70 Rydberg is needed to converge energy differences. This, together with the large vacuum region make standard plane wave based CPMD calculations expensive. For this reason we have decided to use here a novel computational scheme developed in our group.[24,25] In this approach, which we call QUICKSTEP, the Kohn−Sham orbitals are developed in Gaussian-based localized orbitals, while the charge density is expanded in an auxiliary basis set which is a combination of localized and plane wave functions, using some of the ideas of Blöchl.[26] A small number of CPMD calculations[27] will be performed in order to assess the accuracy of the localized basis sets used in the QUICKSTEP calculations. In surface problems a localized basis set approach is particularly well suited since it considerably reduces the cost of describing the vacuum region. Furthermore, using a localized basis set it is possible to describe different regions of space with different accuracy. We shall exploit this fact to enhance the basis set in the crucial region around the catalytic center. In the silica region away from where the chemistry takes place, a smaller basis set can be used.

Our choice has been to use triple-ζ basis sets with two polarization functions for hydrogen (411/11), carbon (555/555/11), and the four oxygen atoms (555/555/11) that interact with the zirconium atom. The latter instead has required a triple-ζ basis set with diffuse s, p, and d functions (6661+/6661+/6661+). The hydrogen atoms on the backside of the slab, which are used only to saturate the dangling bonds, do not require an accurate treatment and have associated a double-ζ basis set with no polarization functions(41). For the rest of the atoms double-ζ basis sets with one polarization function are used (44/44/1). For all atoms other than hydrogen, the basis functions are response function basis sets[28] expanded in primitive Gaussians with shared exponents, that have been optimized for the free atoms. For hydrogen a confining parabolic potential, 0.025 × r^2 (atomic units), is used in the optimization of the exponents.

The two-dimensional Brillouin zones are sampled in the Γ-point only. Using a 2 × 2 point sampling is found to change energy differences by less than 0.5 kcal/mol.

Geometry optimizations for a test molecule [(C_5H_5)$_2$ZrCl_2, bis(η^5-cyclopentadienyl)zirconium dichloride], using both QUICKSTEP and CPMD have been performed. The agreement between the two methods is excellent: bond lengths and angles are the same within 1%. DFT bond lengths and angles agree with the experimental values[29] within 2% except for the Zr−cyclopentadienyl distance which is overestimated by ca. 4%. Using QUICKSTEP we find the Zr−H and Zr−D stretching mode frequencies for ZrH_4 and ZrD_4 molecules to be 1628 and 1160 cm^{-1}, respectively,[30] which is very close to the experimental values[31] (1623.6 and 1166.6 cm^{-1}, respectively).

4. Silica Surfaces

The surface structure of silica surfaces is not well-known, and depends strongly on the preparation and treatments it is subjected to, as for example dehydroxylation. Although the high surface area silicas used as support in catalysis are amorphous, models of the local structure of these surfaces are often based on surfaces of crystalline forms of silica such as β-cristobalite SiO_2[32] and edingtonite,[33] which have atomic densities close to that of amorphous silica. The silicas used in the ≥ZrH experiments have surface areas of ca. 200 m^2/g,[3] corresponding to approximately 100 Å^2 of surface area per 50 SiO_2 units.

DFT gives a good description of the many polymorphs of silica.[34−38] The β-cristobalite polymorph consists of corner-sharing SiO_4 tetrahedra and the structure is determined by two parameters: the lattice constant and the ≥Si−O−Si ≤ angle. A calculation with 16 SiO_2 units, $\vec{k}$-point sampling in the Γ-point only, and our double-ζ basis set gives a lattice constant of 5.17 Å and a ≥Si−O−Si ≤ angle of 150.9° (experiment 5.04 Å and 151.1°).[39] The overestimation of the silica lattice constant (2.5%) is typical for gradient-corrected DFT calculations.[37,38]

A reasonable model describes the silica surface as a mixture of (100) and (111) facets of β-cristobalite.[32] Following this idea we take for our slab calculations the experimental structure of β-cristobalite and cut out an approximately 7 Å thick slab exposing the desired (100) or (111) surfaces. On one side of the slab we saturate the dangling oxygen bonds with hydrogen atoms in order to get OH groups on the surface. On the other side, which we call the backside, the cleaved bonds are also saturated with hydrogens. These hydrogen atoms are not allowed to move in the calculations—this will mimic the constraints that the bulk imposes on the surface. On the (111) surface also the oxygen atoms bonded to the terminal hydrogen atoms are kept fixed during the calculations.

The resulting optimized surfaces are shown in Figures 1a and 2 (we find that the use of very small circles for the oxygen atoms gives the clearest pictures). The relaxations from the "as-cleaved" bulk structure are very small. This is not surprising, since all cleaved bonds are saturated with hydrogen. All silicon atoms coordinate tetrahedrally to four oxygen atoms. On the fully hydroxylated (100) surface (Figure 1a) there are geminal OH groups, >Si(OH)$_2$. Two OH groups on neighboring silicon atoms pointing toward each other are close enough to interact with each other. The two neighboring silicon atoms holding OH groups are separated by ca. 5 Å. After dehydroxylation at 500 °C there are only single isolated OH groups left on the surface.[40] This is in agreement with the formation of siloxane bridges[41] as shown in Figure 1b. These bridges form when two neighboring OH groups combine to release a water molecule. We obtain a dehydroxylated (100) surface from the fully hydrated surface by removing atoms corresponding to one water molecule for each pair of interacting OH groups. The geometry of this surface is then optimized to get the structure shown in Figure 1b with

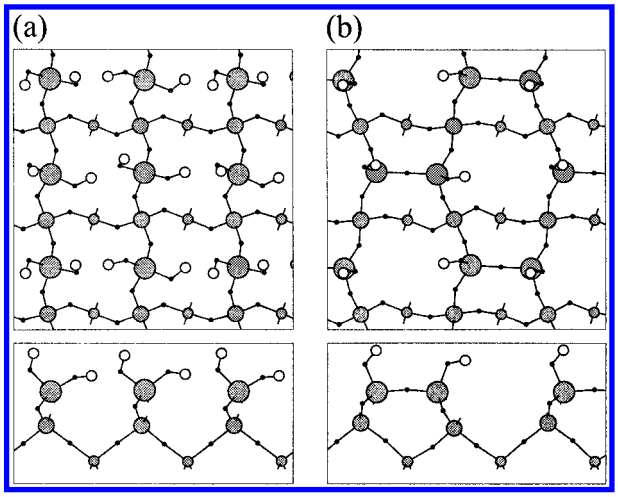

Figure 1. Figure 1. Top and side-view of silica β-cristobalite(100) surface model. Grey circles (Si), small black circles (O), and small white circles (H). (a) Fully hydroxylated surface. (b) Partially dehydroxylated surface. The dangling bonds on the backside of the slabs are saturated with hydrogen atoms (not shown) and kept fixed during the simulation. The sizes of the Si atoms depend on their position: the smaller the circle, the deeper into the substrate is the silicon atom.

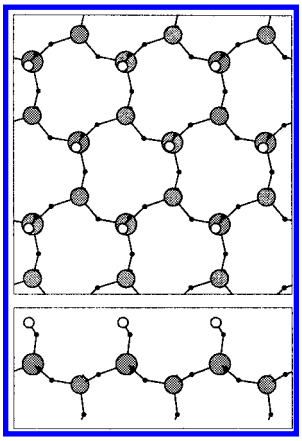

Figure 2. 2. Top and side-view of silica β-cristobalite(111) surface model. Grey circles (Si), small black circles (O), and small white circles (H).

siloxane bridges. We calculate a geminal−geminal dehydroxylation energy of 12 kcal per mol of H_2O (endothermic reaction).

The (111) surface can hold single isolated OH groups as shown in Figure 2. The surface Si−Si distance on this surface is also ca. 5 Å, but here the OH groups are oriented perpendicular to the surface and dehydroxylation is difficult. The OH groups just discussed (Figure 1b and 2) are not the only possibilities. On a real silica surface OH groups can be found at the intersections of facets and at defect sites.[42]

The grafting onto the surface of $ZrNp_4$ (step 1) is strongly exothermic and irreversible (as will be shown later). Therefore, the zirconium will stay at the site where it first reacted. Assuming that all OH groups on the silica surface are equally reactive toward grafting of a $ZrNp_4$ molecule, we expect that the majority of the molecules will be located on the (100) and (111) like patches. We have therefore focused on these two situations.

5. Models for Silica-Supported Zirconium Monohydrides

In the following we will study possible models for the zirconium monohydride catalyst on both the (100) and the (111) surface. Figures 3 and 4 show the surface unit cell

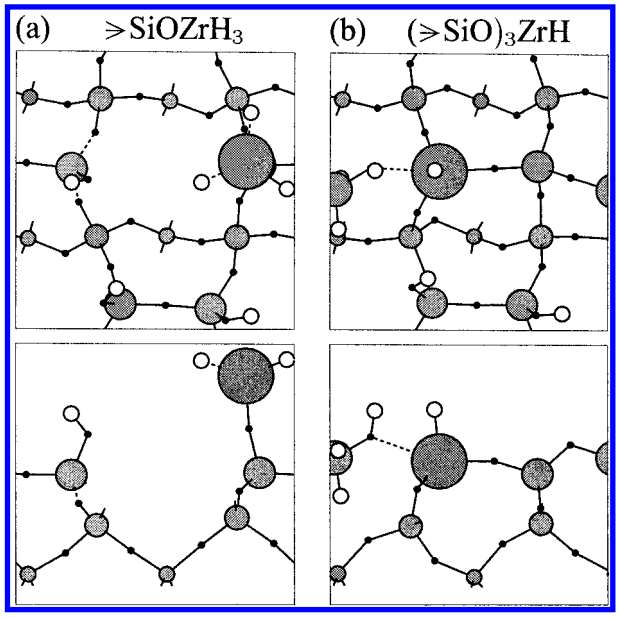

Figure 3. 3. Top and side-view of adsorption of ZrH_4 on the (100) surface. (a) Intermediate state. The bonds that are broken in the formation of the zirconium monohydride are shown dashed. (b) Zirconium monohydride catalyst. The fourth shortest Zr−O bond is shown dashed. Grey circles (Si), small black circles (O), large gray circle (Zr), and small white circles (H).

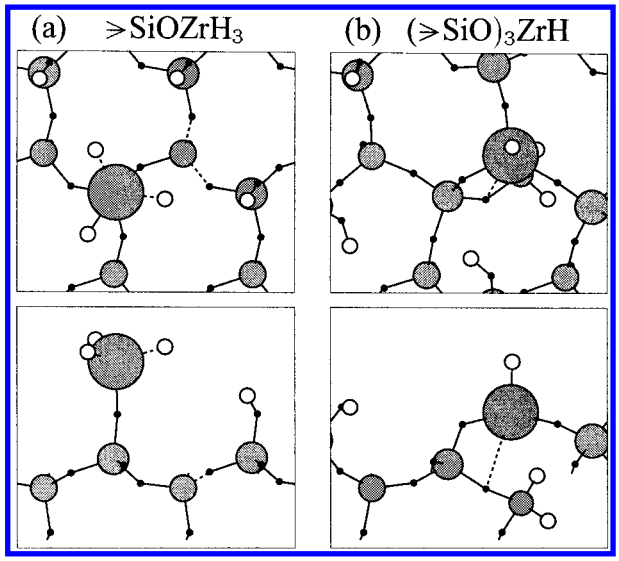

Figure 4. 4. Top and side-view of adsorption of ZrH_4 on the (111) surface. (a) Intermediate state. The bonds that are broken in the formation of the zirconium monohydride are shown dashed. (b) Zirconium monohydride catalyst. The fourth shortest Zr−O bond is shown dashed. Grey circles (Si), small black circles (O), large gray circle (Zr), and small white circles (H).

sizes used in the calculations. We have chosen not to study the detailed dynamic process of the formation of the catalytic center (step 2). Instead, we optimized the geometries for the intermediate state $\geqslant SiOZrH_3$ and for the final state, the zirconium monohydride, and compared their relative energies. The reaction

$$\geqslant SiOH + ZrH_4 \rightarrow \geqslant SiOZrH_3 + H_2 \qquad (3)$$

is found to release an energy of 50 and 53 kcal/mol on the (100) and (111) surfaces, respectively. The next step is the formation of the zirconium monohydride. This reaction is also exothermic. However, for this step there is a big difference between the

two surfaces. On the (100) surface the energy gain is 36 kcal/mol, and on the (111) surface it is 20 kcal/mol. The large energy gain for the reaction

$$\geqslant SiOZrH_3 + (\geqslant SiO)_2Si< \rightarrow (\geqslant SiO)_3ZrH + >SiH_2 \quad (4)$$

on the (100) surface is related to the strained siloxane bridges present on this dehydroxylated surface. By forming the zirconium monohydride, bonds are broken in such a way that the strain of one of the bridges is released (see Figure 3) making the reaction in eq 4 more favorable on the (100) surface compared to on the (111) surface.

The structure of the two model catalysts compare well with EXAFS data[4] for the Zr−O bond lengths (see Table 1). The distance to the three nearest oxygen neighbors is within a few percent of the experimental value. The fourth shortest Zr−O bond (dashed lines in Figures 3b and 4b) has an experimental length of 2.61 Å, which is in very good agreement with our model on the (100) surface (+1%). The corresponding bond length on our (111) surface is much too long. However, one can make a small rearrangement of the substrate which makes the Zr−O bond have a length in better agreement with experiment, but this structure was found to be less reactive toward depolymerization, and will not be described further.

The geometry of the ⩾ZrH site on the (111) surface is very symmetric: the Zr−H bond is very close to perpendicular to the surface. On the (100) surface the angle to the perpendicular direction is ca. 5°.

6. Depolymerization

On the basis of our calculations we find a reaction mechanism which is similar to that proposed by Basset et al.[5] There is, however, an important difference in that we do not find any π-bond between a C═C double bond and the metal−alkyl. This leads us to propose the following modified mechanism.

First the polymer chain is attached to the zirconium atom with liberation of hydrogen:

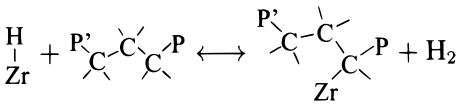

(5)

Here, P and P′ are polymer chains. Next, a β-alkyl is transferred to the metal atom, thereby releasing a polymer chain with a terminal double bond:

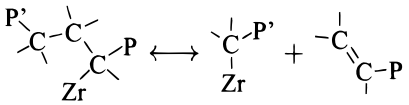

(6)

This is where our proposed mechanism differs from that proposed by Basset et al. (scheme 2 in ref 5). The polymer chain with the terminal double bond is not π-bonded to the metal atom. It is probably an important property of the catalyst that the chain with the terminal double bond (in our calculations an ethylene molecule) is desorbed into the gas phase and not π-bonded to the surface with a strong binding energy. Had this been the case, then there would have been an extra desorption barrier to surmount, making reinsertion of the chain (ethylene molecule) into the zirconium alkyl more favorable (polymerization).

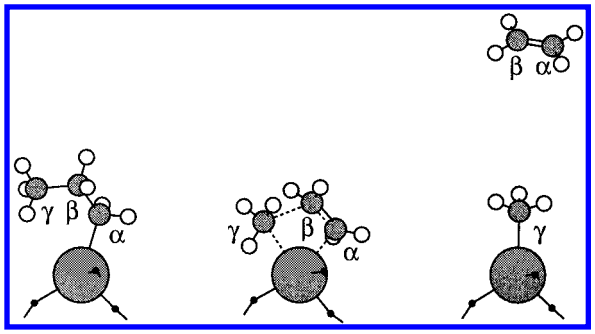

Figure 5. 5. Initial, transition, and final states for β-alkyl transfer to Zr on the (100) surface. Of the substrate, only the three oxygen atoms closest to the zirconium atom are shown.

TABLE 1: Comparison of EXAFS Data from Ref 4 and Our DFT Data for the Zr−O Bondlengths in the Zirconium Monohydride Structure

	coordination number	distance Å
expt	3.1	1.95
	1.1	2.61
DFT (100)	3	1.94, 1.98, 2.01
	1	2.64
DFT (111)	3	1.99, 2.00, 2.01
	(1)	(3.71)

This double bond is then inserted into a zirconium hydrogen bond at another zirconium monohydride site:

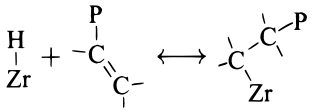

(7)

Finally, the two metal−alkyls are hydrogenated to give the two polymer chain fractions

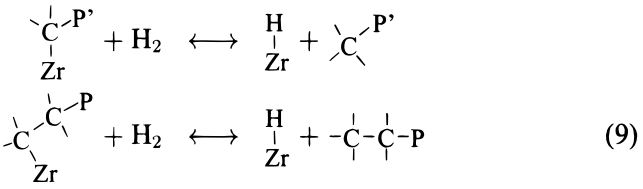

(9)

In the following we will describe the reactions in eqs 5−9 in detail. There are three different types of reactions: β-alkyl transfer, hydrogenolysis, and olefin insertion into a Zr−H bond. The first type is the most important one and has been studied for both the (100) and (111) models, while the later two types of reactions have been investigated only for the (100) model.

***β*-Alkyl Transfer.** We have looked at the shortest polymer (propane) that is known to undergo depolymerization, which corresponds to P, P′ = H in the above equations. Ethane does not have a β-methyl group, and it is therefore inert to the zirconium catalyst. The transition state has a four-center ring structure as shown in Figure 5 for the (100) surface. The transition state is located by optimizing the structure under the constraint of fixed $C_\beta-C_\gamma$ distance ($d_{\beta\gamma}$). The transition state is found at $d_{\beta\gamma} = 2.31$ Å, which is 50% longer than the bond length in the initial state (1.54 Å). The transition state for β-methyl transfer on the (111) surface looks similar, but has $d_{\beta\gamma} = 2.14$ Å. On both surfaces we find that the transition states are stabilized by weak agostic interactions: one of the β-methyl hydrogen atoms is very close to the Zr atom. On the (100) surface the Zr−H distance is 2.40 Å compared to 2.83 Å in the

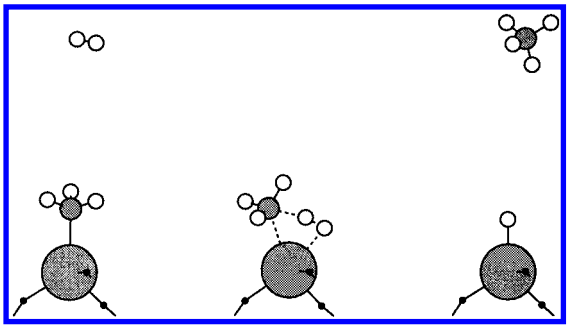

Figure 6. 6. Initial, transition, and final states for hydrogenolysis of $ZrCH_3$ on the (100) surface.

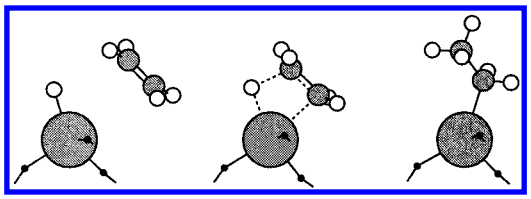

Figure 7. 7. Initial, transition, and final states for insertion of ethylene into a Zr−H bond on the (100) surface.

final state. The C_γ−H bond is also slightly longer (1.11 Å) than the two other C_γ−H bonds (1.09 Å).

Hydrogenolysis. The hydrogenolysis reactions in eqs 8 and 9 and the reverse of eq 5 are all very similar, and we have therefore chosen to study hydrogenation of ≻$ZrCH_3$ on the (100) surface only. The transition state (see Figure 6) is found using the method described above for the β-methyl transfer reaction. In this case a C−H bond length is constrained. The energy barrier for hydrogenation is 13 kcal/mol and the final state (≻ZrH + CH_4) is 11 kcal/mol more stable than the initial state (≻$ZrCH_3$ + H_2). For hydrogenation of zirconium ethyl and zirconium propyl the stabilization energies of the products are 12 and 11 kcal/mol, respectively, on the (100) surface. This indicates that, as we have assumed, these reactions are very similar to the hydrogenation of zirconium methyl, which is the only reaction of the three where we have located the transition state.

Formation of weak complexes between ≻ZrH and methane and between ≻$ZrCH_3$ and H_2 are not observed.

Olefin Insertion into a Zr−H Bond. An ethylene molecule is found to form a weak π-bond to the zirconium hydride (2 kcal/mol). From this state it inserts into the Zr−H bond on the (100) surface, over a very small barrier of 2 kcal/mol (the initial, transition, and final states are shown in Figure 7). The reaction is exothermic, releasing an energy of 22 kcal/mol.

7. Potential Energy Surface for Depolymerization on the (100) Surface

We are now ready to construct an energy diagram for the complete depolymerization mechanism on our (100) surface model. In Figures 8 and 9 the zero of energy is at the initial state, which is the zirconium monohydride plus H_2 and propane (the polymer) in the gas phase. The final state that we want to arrive at is methane and ethane (the two polymer fractions) plus the zirconium monohydride that we started from. The overall depolymerization reaction is exothermic by 20 kcal/mol (the experimental value for the reaction $C_2H_6 + H_2 \rightarrow 2CH_4$ is 18 kcal/mol,[43] but before the products are formed, a number of barriers must be crossed. The first barrier to overcome is the binding of the polymer (propane molecule) to the Zr atom, with the release of hydrogen. Then the β-methyl group is transferred

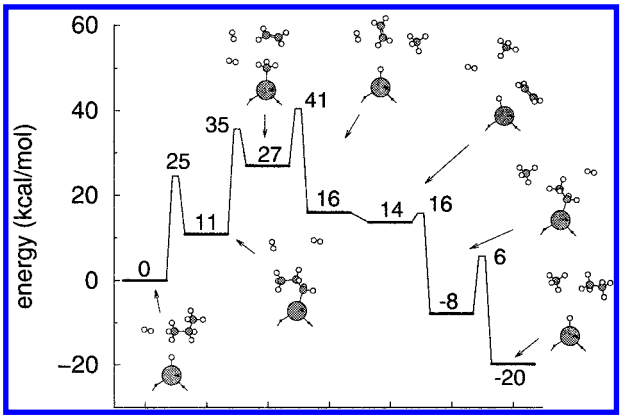

Figure 8. 8. Energy diagram for depolymerization of propane on a single zirconium monohydride site on a (100) surface. The zero of energy is the zirconium monohydride plus propane and hydrogen in the gas phase. Zero-point energies are not included. The numbers on the graph give the energies (in kcal/mol) for all stable states and transition states.

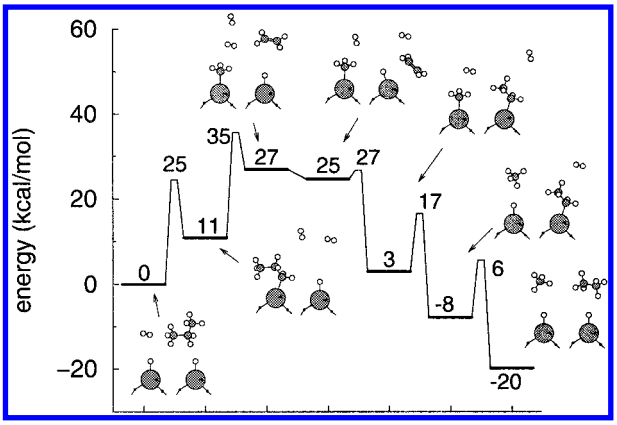

Figure 9. 9. Energy diagram for depolymerization of propane on a (100) surface using two zirconium monohydride sites. The numbers on the graph give the energies (in kcal/mol) for all stable states and transition states.

to the Zr atom. Once the C_β−C_γ bond has been broken we have a zirconium methyl and a free ethylene molecule (see eq 6).

From here on the reaction can proceed in two different ways: (1) Figure 8 shows the route, that must be followed if the density of vacant ≻ZrH sites is low. Then the zirconium methyl must be hydrogenolyzed first, to free a ≻ZrH site that can be used to insert the ethylene molecule into. Hydrogenolysis of the zirconium ethyl species then leads to the desired final state. (2) If there are enough vacant ≻ZrH sites available then the ethylene molecule can insert into one of these Zr−H bonds. This is then followed by hydrogenolysis of the zirconium methyl and ethyl. This mechanism is shown in Figure 9, and the activation energy will be

$$\Delta E = E(\succ ZrC_3H_7^{\#}) + E(H_2) - E(\succ ZrH) - E(C_3H_8) \quad (10)$$

This second route has a lower activation energy compared to the first route (35 and 41 kcal/mol, respectively). It is therefore important that a polymer attached to a zirconium atom is not too stable compared to ≻ZrH. If the polymers attached to the zirconium sites are very stable, then the catalyst would quickly deactivate; if the equilibrium in eq 5 is too far to the right then the activation energy will be larger, because of the energy required to create new vacant ≻ZrH sites. For this reason, depolymerization is often performed at very high H_2 pressures,[1,44] which will shift the equilibrium to higher ≻ZrH

densities. For our model catalyst there seems to be no need to operate at high H_2 pressures, in agreement with the experimental observations.

On the (111) surface we find the barrier for β-methyl transfer to be much higher than on the (100) surface (47 and 35 kcal/mol, respectively). These numbers do not include zero-point energies. Including this correction, we find a barrier of 29 kcal/mol on the (100) surface (see next paragraph).[45] Since we also found the zirconium monohydride to be less stable on the (111) surface compared to the (100) surface, we expect that the zirconium sites on the (100) surface will dominate the catalytic activity completely.

A normal-mode analysis was performed on the transition state shown in Figure 5 for the β-methyl transfer step on the (100) surface. In this analysis the heavy zirconium atom and the substrate are fixed. We find exactly one imaginary frequency ($135i$ cm^{-1}) with a normal mode that corresponds to a breaking of the $C_\beta-C_\gamma$ and $Zr-C_\alpha$ bonds and a formation of the $Zr-C_\gamma$ bond. This confirms the validity of the procedure followed to locate the transition state. From the calculated frequencies we get an estimate of the zero-point energy in the harmonic approximation.

If the rate-limiting step is the β-methyl transfer reaction (eq 6), then the activation energy for depolymerization will be as defined in eq 10. The zero-point energy corrections to this activation energy barrier is -6 kcal/mol giving $\Delta E = 29$ kcal/mol. Part of this large correction comes from the degree of freedom missing in the transition state—this degree of freedom is the $C_\beta-C_\gamma$ stretch mode which has a large frequency. The rest of the correction must come from a softening of the normal modes of the transition state compared to the initial state.

Our two model catalysts have activation energies that differ by ca. 12 kcal/mol. The difference is caused by differences in the local environment of the zirconium atom. We expect that there will be a number of other environments different from the two we have studied on highly ordered single-crystal surfaces. We believe that the zirconium centers on the real catalyst will have a distribution of activation energies for the different steps involved in depolymerization such as hydrogenation and β-alkyl transfer. Our calculations suggest that strained silica rings, which are present on amorphous silica surfaces[46,47] and also on our dehydroxylated (100) surface model, are important.

8. Conclusion

We have studied two different models of a silica surface, both cut from the β-cristobalite SiO_2 bulk structure, with dangling bonds saturated with hydrogen atoms. On the (100) surface of β-cristobalite, the silanol density is reduced by a factor of 2 by desorbing water and forming siloxane bridges. The OH groups on these surfaces are found to react similarly and strongly with ZrH_4 to form H_2 and a surface species where the Zr atom is singly coordinated to an oxygen atom. The formation of a 3-fold coordinated zirconium monohydride is found to be more favorable on the (100) surface than to on the (111) surface. On both surfaces the structure of the zirconium monohydride is in very good agreement with the experimentally determined structure.

For these two model catalysts we have studied the steps involved in depolymerization of a small model polyolefin, namely propane. The products of this reaction are methane and ethane. The effective activation energy we find for the reaction on a β-cristobalite (100) surface is 29 kcal/mol. The value for the (111) surface is approximately 12 kcal/mol higher. The rate-limiting step is a β-methyl transfer to the zirconium atom. This is the microscopic inverse of a Ziegler−Natta (ZN) polymerization step: insertion of ethylene into the zirconium alkyl bond. There is one important difference, however. The ethylene molecule does not make a strong π-bond to $\geqslant ZrCH_3$ as is the case for ZN catalysts. This will disfavor reinsertion of the ethylene molecule into the zirconium methyl bond, which is important for a good depolymerization catalyst.

Another important property of the silica-supported zirconium monohydride catalyst is that the equilibrium $\geqslant ZrC_nH_{2n+1} + H_2 \leftrightarrow \geqslant ZrH + C_nH_{2n+2}$ is so much to the right, that the catalyst is never self-deactivated by polymer chains, making high H_2 pressures unnecessary.

Supporting Information Available: The structures shown in Figures 1−7 are available as Protein Data Bank files (PDB format). This material is available free of charge via the Internet at http://pubs.acs.org.

References and Notes

(1) Shabtai, J.; Xiao, X.; Zmierczak, W. *Energy Fuels* **1997**, *11*, 76.
(2) Shabtai, J.; Ramakrishnan, R.; Oblad, A. G. *Thermal Hydrocarbon Chemistry*; Advances in Chemistry Series 183, American Chemical Society: Washinton, DC, 1979; Chapter 18, p 297.
(3) Quignard, F.; Lécuyer, C.; Choplin, A.; Olivier, D.; Basset, J.-M. *J. Mol. Catal*. **1992**, *74*, 353.
(4) Corker, J.; Lefebvre, F.; Lécuyer, C.; Dufaud, V.; Quignard, F.; Choplin, A.; Evans, J.; Basset, J.-M. *Science* **1996**, *271*, 966.
(5) Dufaud, V.; Basset, J.-M. *Angew. Chem., Int. Ed. Engl*. **1998**, *37*, 806.
(6) Korányi, T. I.; Magni, E.; Somorjai, G. A. *Top. Catal*. **1999**, *7*, 179.
(7) Margl, P.; Lohrenz, J. C. W.; Ziegler, T.; Blöchl, P. E. *J. Am. Chem. Soc*. **1996**, *118*, 4434.
(8) Kawamura-Kuribayashi, H.; Koga, N.; Morokuma, K. *J. Am. Chem. Soc*. **1992**, *114*, 8687.
(9) Puhakka, E.; Pakkanen, T. T.; Pakkanen, T. A. *Surf. Sci*. **1995**, *334*, 289.
(10) Cavallo, L.; Guerra, G.; Corradini, P. *J. Am. Chem. Soc*. **1998**, *120*, 2428.
(11) Lin, J. S.; Catlow, C. R. A. *J. Catal*. **1995**, *157*, 145.
(12) Boero, M.; Parrinello, M.; Terakura, K. *J. Am. Chem. Soc*. **1998**, *120*, 2746.
(13) Boero, M.; Parrinello, M.; Hüffer, S.; Weiss, H. First principles study of propene polymerization in Ziegler−Natta heterogeneous catalysis. Submitted.
(14) Moore, E. P., Jr., Ed.; *Polypropylene Handbook*; Hanser Publishers, Munich, Vienna, New York, 1996.
(15) Hohenberg, P.; Kohn, W. *Phys. Rev*. **1964**, *136*, B864.
(16) Kohn, W.; Sham, L. *Phys. Rev. A* **1965**, *140*, 1133.
(17) Feuston, B. P.; Garofalini, S. H. *J. Appl. Phys*. **1990**, *68*, 4830.
(18) Branda, M. M.; Castellani, N. J. *Surf. Sci*. **1997**, *393*, 171.
(19) Becke, A. D. *Phys. Rev. A* **1988**, *38*, 3098.
(20) Lee, C.; Yang, W.; Parr, R. G. *Phys. Rev. B* **1988**, *37*, 785.
(21) Goedecker, S.; Teter, M.; Hutter, J. *Phys. Rev. B* **1996**, *54*, 1703.
(22) Hartwigsen, C.; Goedecker, S.; Hutter, J. *Phys. Rev. B* **1998**, *58*, 3641.
(23) Martyna, G. J.; Tuckerman, M. E. *J. Chem. Phys*. **1999**, *110*, 2810, For a 2D slab geometry, the screening function defined by Martyna and Tuckerman can be given in an analytic form. With C being the height of the cell, and $\vec{G} = \{g \cos\theta, g \sin\theta, g_z\}$ a reciprocal space vector, where $g_z = n_z(2\pi/C)$ and n_z is an integer, we get:

$$\hat{\phi}_{2D}^{(screen)}(\vec{G}) = -\frac{4\pi}{G^2}(-1)^{n_z} e^{-gC/2}$$

See also [G. J. Martyna, K. Pihakari, M. E. Tuckerman (to be published)].
(24) Lippert, G. *Die GAPW-Dichtefunktional-Methode für Ab Initio Molekulardynamik-Simulationen*. Ph.D. Thesis. Max-Planck-Institut für Festkörperforschung, 1998.
(25) Lippert, G.; Hutter, J.; Parrinello, M. *Mol. Phys*. **1997**, *92*, 477.
(26) Blöchl, P. E. *Phys. Rev. B* **1994**, *50*, 19753.
(27) The CPMD code we have used, was developed by J. Hutter, P. Ballone, M. Bernasconi, P. Focher, E. Fois, S. Goedecker, D. Marx, M. Parrinello, and M. Tuckerman, at MPI für Festkörperforschung and IBM Zurich Research Laboratory (1990−1997).
(28) Lippert, G.; Hutter, J.; Ballone, P.; Parrinello, M. *J. Phys. Chem*. **1996**, *100*, 6231.

(29) Ronova, I. A.; Alekseev, N. V. *J. Struct. Chem.* **1977**, *18*, 180.
(30) The calculated potential is fitted to a Morse potential. The nuclear Schrödinger equation can then be solved exactly for this anharmonic potential to give the energy difference between the first excited state and the ground state.
(31) Chertihin, G. V.; Andrews, L. *J. Am. Chem. Soc.* **1995**, *117*, 6402.
(32) Chuang, I.-S.; Maciel, G. E. *J. Phys. Chem. B* **1997**, *101*, 3052.
(33) Civalleri, B.; Casassa, S.; Garrone, E.; Pisani, C.; Ugliengo, P. *J. Phys. Chem. B* **1999**, *103*, 2165.
(34) Allan, D. C.; Teter, M. P. *Phys. Rev. Lett.* **1987**, *59*, 1136.
(35) Chelikowsky, J. R.; H. E. King, J.; Troullier, N.; Martins, J. L.; Glinnemann, J. *Phys. Rev. Lett.* **1990**, *65*, 3309.
(36) Liu, F.; Garofalini, S. H.; King-Smith, F.; Vanderbilt, D. *Phys. Rev. B* **1994**, *49*, 12528.
(37) Hamann, D. R. *Phys. Rev. Lett.* **1996**, *76*, 660.
(38) Zupan, A.; Blaha, P.; Schwarz, K.; Perdew, J. P. *Phys. Rev. B* **1998**, *58*, 11266.
(39) Wright, A. F.; Leadbetter, A. J. *Philos. Mag.* **1975**, *31*, 1391.
(40) Rosier, C.; Niccolai, G. P.; Basset, J.-M. *J. Am. Chem. Soc.* **1997**, *119*, 12408.
(41) Sindorf, D. W.; Maciel, G. E. *J. Am. Chem. Soc.* **1983**, *105*, 1487.
(42) Chiang, C.-M.; Zegarski, B. R.; Dubois, L. H. *J. Phys. Chem.* **1993**, *97*, 6948.
(43) Pople, J. A.; Head-Gordon, M.; Fox, D. J.; Raghavachari, K.; Curtiss, L. A. *J. Chem. Phys.* **1989**, *90*, 5622.
(44) Garin, F.; Andriamasinoro, D.; Abulsamad, A.; Sommer, J. *J. Catal.* **1991**, *131*, 199.
(45) The energy barrier changed by less than 2 kcal/mol when calculated with a planewave basis set.
(46) King, S. V. *Nature* **1967**, *213*, 1112.
(47) Hamann, D. R. *Phys. Rev. B* **1997**, *55*, 14784.